EKF-based scaling factor identification for strap-down seeker

Wang Wei, Ji Yi, Shi Zhongjiao, Lin Defu, Lin Shiyao

(School of Aerospace Engineering, Beijing Institute of Technology, Beijing 100081, China)

Abstract: Based on extended Kalman filter (EKF), a scaling factor (SF) identification method for strap-down seeker (SS) was proposed. First, a nonlinear model for SS system was set up under proportional guidance (PNG) law. Then, the extended Kalman equations were deduced on this nonlinear model, and it should be linearized at the value of EKF estimated based on Taylor expansion. At last, actions of this method on how to keep guidance system stability were studied under above conditions. According to mathematic simulation results, in this way, the SSSF could be estimated accurately and quickly, and the tolerable SSSF error scope of guidance system stability is extended, the robustness of system is promoted.

Key words: strap-down seeker; extended Kalman filter; scaling factor; identification

CLC number: TJ765 **Document code:** A **DOI**: 10.3788/IRLA201746.0417003

基于扩展卡尔曼滤波器的捷联导引头刻度尺参数辨识

王 伟，纪 毅，石忠佼，林德福，林时尧

(北京理工大学 宇航学院，北京 100081)

摘 要：基于扩展卡尔曼滤波器，提出一种捷联导引头刻度尺参数辨识方法。首先，简化了在比例导引制导律作用下捷联导引头系统的非线性模型。之后，根据该非线性模型，推导扩展卡尔曼滤波方程组，并在参数估计处利用泰勒展式将其线性化。最后，在以上条件下对制导系统的稳定性进行理论分析与研究。通过数学仿真对该刻度尺参数辨识方法加以验证，仿真结果表明：应用该方法，可以快速、准确的估计捷联导引头刻度尺参数，并且有效提高了在稳定性方面制导系统对导引头刻度尺系数误差的容忍度，使系统更具鲁棒性。

关键词：捷联导引头； 扩展卡尔曼滤波； 刻度尺系数； 辨识

收稿日期：2016-08-05； **修订日期：**2016-09-15

作者简介：王伟(1984-)，男，实验师，硕士生导师，主要从事关于飞行器总体设计与控制工程、武器系统工程方面的研究。
Email:wangweiyh@bit.edu.cn

通讯作者：纪毅(1984-)，男，硕士生，主要从事关于飞行器总体设计与控制工程方面的研究。Email: yijiinbit@163.com

0 Introduction

Technology of strap-down seeker(SS) has attracted many powers around the word in the past few years. Comparing with traditional seekers, smaller volume, lower cost, higher reliability and other advantages made the unshakeable dominance of SS in its own field [1]. However, line-of-sight (LOS) angle must be acquired firstly in order to achieve SS's engineering application, and attitude gyro, usually, is employed to decouple the missile's attitude angles[2].

Generally, only the coupling angular motion error angle could be measured because SS which is fixed on the missile cannot measure LOS angle directly. SF error could be introduced in a parasitic loop, perhaps results in unstable, if the accuracy of SF was considered less importantly[3]. It is different from the gimbal seeker's scale error, which only leads the change of guidance parameters.

Disturbance rejection will be induced by SF error of the seeker, at the same time, parasitic loop will also be induced. Related stable region is caused by disturbance rejection and parasitic loop[4]. The outside loop of guidance system will intensify the influence of the parasitic loop, because the effective distance of the seekers is limited and the parasitic loop has important effect on the strap-down guidance system. Different stable regions and feedback characters are determined by the error of SF. The Identification of SF and the compensation of SF error could help improve the stability and the guidance accuracy[5]. Hence, it is important to identify SSSF.

Now, there are only a few researches about the identification of SSSF. Willman W W[6] detailed the estimation about SF through adding a fluctuating acceleration component in the feedback. Zarchan P and Gratt H[7] came up with the adaptive radome compensation using dither to identify the SF parameters. Li F, et al[8] and Du, et al[9] presented an autoregressive identification method by ignoring the time constant of the seeker and the gyro, but a big error still exists in. Zong R, et al[10] proposed a real time compensation method for scale factor error based on unscented Kalman filter, and points out that both of missile system stability and guidance accuracy are improved after the compensation. Zheng D, et al[11] analyses the reason of disturbance rejection parasitic loop in SS, and establishes the model of SF error. Wang L, et al [12] studied the effects of noise and SF error existing in SS on guidance system performance, and points out that relative change of SF error has bigger influence on impact accuracy. Wang Z [13], Ananthasayanam M R, et al [14] and Smita Sadhu, T K Ghoshal [15] proposed some methods about how to estimate LOS rates and angles with EKF respectively.

In this paper, an identification method based on EKF is proposed, and there is significant influence on the guidance system through the study in some cases.

1 Strap-down seeker's model

The block diagram of proportional navigation guidance system based on SS is illustrated in Fig.1 [16]. Where, $1/Ts+1$ is employed to describe the dynamic lag of guidance system; the transfer function of the missile control system is expressed as $1/T_m^2 s^2+2T_m\mu_m s+1$. X_1-X_7, seven variables are involved in the navigation model, which represent the LOS angle q, the LOS angle rate $\dot{q}$, the output LOS angle rate by lag phase $\dot{q}_d$, the first order derivative of normal overload with respect to time t $\dot{a}_m$, the normal overload a_m, the normal velocity v_m and the seeker's scale factor k_s. Two measurement parameters, Z_1 and Z_2, are employed to describe the error output angle of the seeker and attitude angles obtained by attitude gyro respectively. The measurement noises of the two parameters are expressed as V_1 and V_2. In this paper, the usual assumption corresponding to seeker's model is adopted, the measurement noises and the system interfering noises (w_2) are white noise. Some symbols are also adopted to describe the mathematical model. t_F , the end time of guidance; t , the flight time;

k_g, the scale factor of attitude gyro; v, the relative velocity between target and missile; ϑ, the attitude angle of missile; $\hat{\dot{q}}$, the LOS angle rate estimated by extended Kalman filter.

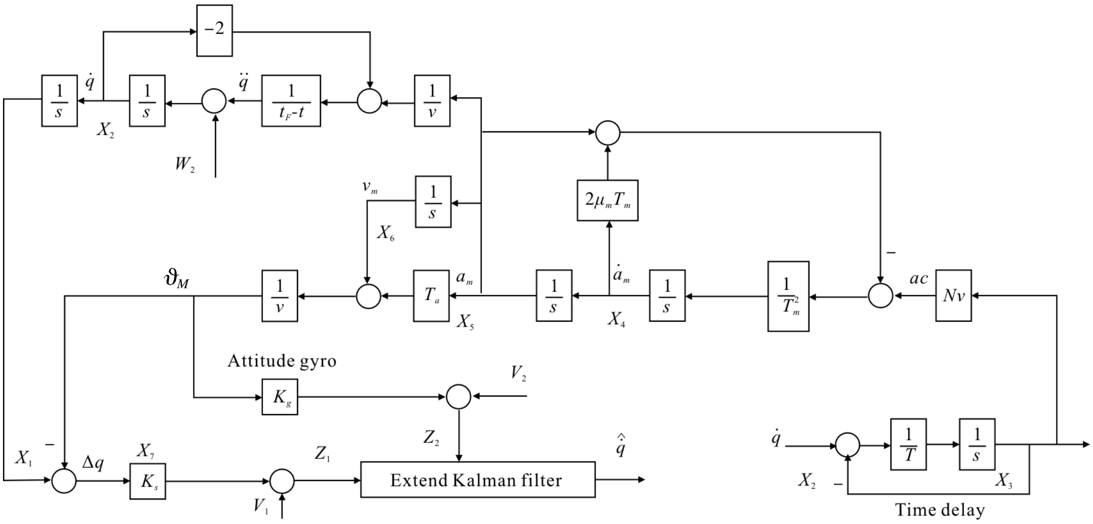

Fig.1 Proportional navigation guidance system block diagram based on strap-down seeker

The system statement equations obtained from Fig.1 could be expressed as Eq.(1):

$$\begin{cases}\dot{X}_1=X_2\\ \dot{X}_2=-\dfrac{1}{(t_F-t)}(-2X_2+\dfrac{X_5}{v})+w_2\\ \dot{X}_3=-\dfrac{1}{T}(X_2-X_3)\\ \dot{X}_4=-\dfrac{1}{T_m^2}(NvX_3-2\mu_m T_m X_4-X_5)\\ \dot{X}_5=X_4\\ \dot{X}_6=X_5\\ \dot{X}_7=w_7\end{cases}\quad(1)$$

Eqation(2) describes the measurement equations:

$$\begin{cases}Z_1=X_7(X_1-\dfrac{1}{v}X_6-\dfrac{T_\alpha}{v}X_5)+V_1\\ Z_2=k_g(\dfrac{1}{v}X_6+\dfrac{T_\alpha}{v}X_5)+V_2\end{cases}\quad(2)$$

2 Linear equations of EKF

2.1 Principle of EKF

Assuming that the nonlinear stochastic system could be expressed as:

$$\begin{cases}\dot{X}(t)=\varphi[X(t),t]+F[X(t),t]W(t)\\ Z(t)=h[X(t),t]+V(t)\end{cases}$$

New equations could be obtained by expanding the nonlinear model based on Taylor expansion and omitting the second and higher order items:

$$\begin{cases}\dot{X}(t)=\varphi[\hat{X}(t|t),t]+\left.\dfrac{\partial\varphi[X(t),t]}{\partial X(t)}\right|_{X(t)=\hat{X}(t|t)}[X(t)-\hat{X}(t|t)]+F[X(t),t]+W(t)\\ Z(t)=h[\hat{X}(t|t),t]+\left.\dfrac{\partial h[X(t),t]}{\partial X(t)}\right|_{X(t)=\hat{X}(t|t)}[X(t)-\hat{X}(t|t)]+V(t)\end{cases}$$

In order to provide a succinct method of writing the mathematical equations in this paper, some definitions are employed:

$$\left.\frac{\partial\varphi[X(t),t]}{\partial X(t)}\right|_{X(t)=\hat{X}(t|t)}=A(t)$$

$$\varphi[\hat{X}(t|t),t]-A(t)\hat{X}(t|t)=U(t)$$

$$\left.\frac{\partial h[X(t),t]}{\partial X(t)}\right|_{X(t)=\hat{X}(t|t)}=H(t)$$

$$h[\hat{X}(t|t),t]-H(t)\hat{X}(t|t)=Y(t)$$

$F[X(t),t]$ could be written as:

$$F[\hat{X}(t|t),t]\triangleq F(t)$$

so new equations could be expressed as follow:

$$\begin{cases}\dot{X}(t)=A(t)X(t)+U(t)+F(t)W(t)\\ Z(t)=H(t)X(t)+Y(t)+V(t)\end{cases}$$

The EKF equation in continuous style is:

$$\hat{X}(t|t)=A(t)\hat{X}(t|t)+K(t)[Z(t)-Y(t)-H(t)\hat{X}(t|t)]+U(t)$$

Substituting $Y(t)$, $U(t)$ into the above equation, yields:

$$\dot{X}(t|t)=\varphi[\hat{X}(t|t),t]+K(t)\{Z(t)-h[\hat{X}(t|t),t]\}$$

So the continuous EKF equations could be expressed as[4]:

$$\hat{X}(t|t)=\varphi[\hat{X}(t|t),t]+K(t)\{Z(t)-h[\hat{X}(t|t),t]\} \quad (3)$$

$$K(t)=P(t|t)H^{T}(t)R^{-1}(t) \quad (4)$$

$$\dot{P}(t|t)=A(t)P(t|t)+P(t|t)A^{T}(t)-P(t|t)H^{T}(t)R^{-1}(t)H(t)P(t|t)+F(t)Q(t)F^{T}(t) \quad (5)$$

2.2 Linear equations

In order to adapt EKF, the state equations and the observation equations of system have to be linearized. The results of Eq. (1) and Eq. (2) linearization could be expressed as follows:

$$\begin{cases}\dot{X}(t)=A(t)X(t)+U(t)+F(t)W(t)\\ Z(t)=H(t)X(t)+Y(t)+V(t)\end{cases}$$

Using Taylor expansion and omitting second-order values and other higher order values, then, taking the partial derivatives of the state values in the state equations, some items are expressed as follows:

$$A(t)=\frac{\partial\varphi[X(t),t]}{\partial X(t)}\Big|_{X(t)=\hat{X}(t|t)}=\begin{bmatrix}0&1&0&0&0&0&0\\0&\frac{2}{t_F-t}&0&0&-\frac{1}{(t_F-t)v}&0&0\\0&\frac{1}{T}&-\frac{1}{T}&0&0&0&0\\0&0&\frac{Nv}{T_m^2}&-\frac{2\mu_m}{T_m}&-\frac{1}{T_m^2}&0&0\\0&0&0&1&0&0&0\\0&0&0&0&1&0&0\\0&0&0&0&0&0&0\end{bmatrix}$$

$$U(t)=\varphi[\hat{X}(t|t),t]-A(t)\hat{X}(t|t)=0$$

Taking the partial derivatives of the state values in observation equations, then, some items are express as follows:

$$H(t)=\frac{\partial h[X(t),t]}{\partial X(t)}\Big|_{X(t)=\hat{X}(t|t)}=\begin{bmatrix}\hat{X}_7(t|t)&0&0&0&-\frac{T_\alpha}{v}\hat{X}_7(t|t)&-\frac{\hat{X}_7(t|t)}{v}&[\hat{X}_1(t|t)-\frac{1}{v}\hat{X}_6(t|t)-\frac{T_\alpha}{v}\hat{X}_5(t|t)]\\0&0&0&0&\frac{T_\alpha}{v}k_g&\frac{k_g}{v}&0\end{bmatrix}$$

$$Y(t)=h[\hat{X}(t|t),t]-H(t)\hat{X}(t|t)=\begin{bmatrix}-[\hat{X}_1(t|t)-\frac{1}{v}\hat{X}_6(t|t)-\frac{T_\alpha}{v}\hat{X}_5(t|t)]\hat{X}_7(t|t)\\0\end{bmatrix}$$

Where, $A(t)$ is the state equations′ partial derivative by $X(t)$, $H(t)$ is the observation equations′ partial derivative by $X(t)$. Now, identify $F(t)$ is a seven-dimension unit matrix, thus,

$$F(t)=\begin{bmatrix}1&0&0&0&0&0&0\\0&1&0&0&0&0&0\\0&0&1&0&0&0&0\\0&0&0&1&0&0&0\\0&0&0&0&1&0&0\\0&0&0&0&0&1&0\\0&0&0&0&0&0&1\end{bmatrix},X=\begin{bmatrix}X_1\\X_2\\X_3\\X_4\\X_5\\X_6\\X_7\end{bmatrix},W=\begin{bmatrix}0\\w_2\\0\\0\\0\\0\\w_7\end{bmatrix},$$

$$Z(t)=\begin{bmatrix}Z_1(t)\\Z_2(t)\end{bmatrix},V(t)=\begin{bmatrix}V_1(t)\\V_2(t)\end{bmatrix}。$$

3 Simulation

3.1 Identification of seeker scale factor

Assuming that the nominal value of the seeker scale factor is 1.0, and make it equal to the initial value of EKF. Simulations are performed when the real SF is 1.5 and 0.5 respectively. Some parameters′ values are presented as: T=0.02 s, N=3, v=220 m/s, μ_m=0.1, T_m=0.08 s, T_α=1.6 s, k_g=1.0, t_F=20 s。

The initial value of EKF is:

$$\hat{X}(0)=[0\ \ 0\ \ 0\ \ 0\ \ 0\ \ 0\ \ 1.0]^{T}$$

$$P(0|0)=\begin{bmatrix} 0 & 0 & 0 & 0 & 0 & 0 & 0 \\ 0 & 0.001\ 218 & 0 & 0 & 0 & 0 & 0 \\ 0 & 0 & 0 & 0 & 0 & 0 & 0 \\ 0 & 0 & 0 & 0 & 0 & 0 & 0 \\ 0 & 0 & 0 & 0 & 0 & 0 & 0 \\ 0 & 0 & 0 & 0 & 0 & 0 & 0 \\ 0 & 0 & 0 & 0 & 0 & 0 & 0.25 \end{bmatrix}$$

The system′s interfering noise matrix of power spectral density is:

$$Q=\begin{bmatrix} 0 & 0 & 0 & 0 & 0 & 0 & 0 \\ 0 & 3.046\times10^{-6} & 0 & 0 & 0 & 0 & 0 \\ 0 & 0 & 0 & 0 & 0 & 0 & 0 \\ 0 & 0 & 0 & 0 & 0 & 0 & 0 \\ 0 & 0 & 0 & 0 & 0 & 0 & 0 \\ 0 & 0 & 0 & 0 & 0 & 0 & 0 \\ 0 & 0 & 0 & 0 & 0 & 0 & 2.5\times10^{-7} \end{bmatrix}$$

The measurement noise matrix of power spectral density is:

$$R=\begin{bmatrix} 1.218\times10^{-8} & 0 \\ 0 & 1.218\times10^{-8} \end{bmatrix}$$

The simulation result is showed in Fig.2 at the circumstance of the initial value is:

$$X(0)=[0\quad 0.034\ 9\ 0\ 0\ 0\ 0\ 1.5]^{T}$$

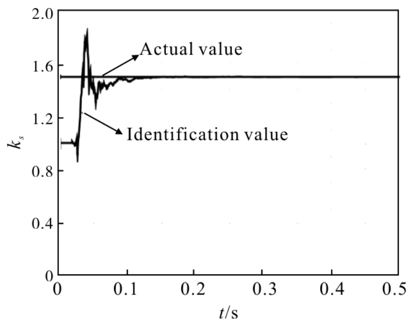

Fig.2 Curves of scaling factor real value and identification value (real value has +50% error)

It can be summarized from Fig.2 that EKF filter can identify the real SF instantly when the real SF is bigger than the nominal SF by 50%.

The simulation result is showed in Fig.3 at the circumstance of the initial value is:

$$X(0)=[0\quad 0.034\ 9\ 0\ 0\ 0\ 0\ 0.5]^{T}$$

It can be summarized from Fig.3 that EKF can identify the real SF instantly when the real SF is smaller than the nominal SF by 50%.

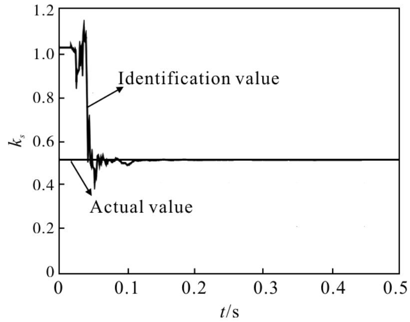

Fig.3 Curves of scaling factor real value and identification value (Real value has −50% error)

3.2 Decouple effect of identify method

Three curves are illustrated in Fig.4 at the circumstances of ±10% real SF error, 0.034 9(°)/sinitial LOS angle rate without EKF and PN guidance law. Contrasting with no SF error and initial angle rate curve, it can be seen that the system will be unstable at the circumstance of ±10% real SF error without EKF. The result with the same error and EKF is shown in Fig.5, only ±10% errors exist in SF after filtering by EKF, which has less influence on the guidance system.

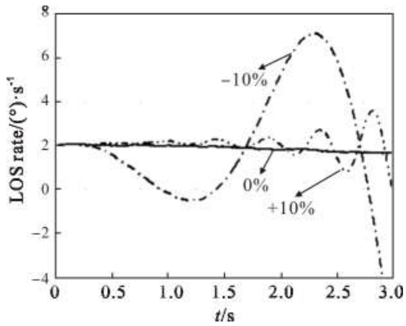

Fig.4 Curve of line-of-sight rate (no parameter identification)

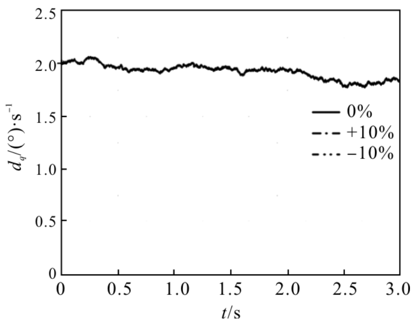

Fig.5 Curve of line-of-sight rate (parameter identification)

4 Conclusions

The guidance system model of PN based on SS is established in this paper. Meanwhile, EKF is employed to identify SSSF. It is proved that the method presented in this paper could identify the scale factor instantly and accurately through the simulation. It is also validated that the SF identified by EKF could help improve the tolerant range, which the stability of guidance system to the SSSF error.

References:

[1] Yao Y, Zhang G. Discussion on strap-down imaging guidance system [J]. ***Infrared and Laser Engineering***, 2006, 35(1): 1-6. (in Chinese)

[2] Zhou R. Stabilization and Tracking Technology of Strap-down Seeker [M]. Beijing: National Defence Industry Press, 2010. (in Chinese)

[3] Thomas C, Callen R. Guidance law design for tactical weapons with strap-down seekers [C]//AIAA, Guidance & Control Conderence, 2013.

[4] Wang W, Lin D, Xv P. Disturbance rejection program induced by strap-down seeker time delay [J]. ***Infrared and Laser Engineering***, 2015, 44(9): 2854-2857. (in Chinese)

[5] Yuan Y. Research on guidance and control technology for strapdown guided munition [D]. Beijing: Beijing Institute of Technology, 2014. (in Chinese)

[6] Willman W W. Effects of strap-down seeker scale-factor uncertainty on optimal guidance [J]. ***Journal of Guidance, Control, and Dynamics***, 1988, 11(3): 199-206.

[7] Zarchan P, Gratt H. Adaptive radome compensation using dither [J]. ***Journal of Guidance, Control, and Dynamics***, 1999, 22(1): 51-57.

[8] Li F, Xia Q, Qi Z. Effect of parasitic loop on strap-down seeker and compensated with identification method [J]. ***Systems Engineering and Electronics***, 2013, 35(8): 1717-1722. (in Chinese)

[9] Du Y, Xia Q, Guo T. Study on stability of strap-down seeker scale factor error parasitical loop [C]// Computer, Mechatronics, Control and Electronic Engineering, 2010 International Conference on IEEE, 2010, 6: 55-58.

[10] Zong R, Lin D, Liu T, et al. Compensation method fro scale error of optical strapdown seeker using UKF [J]. ***Infrared and Laser Engineering***, 2014, 43(11): 3577-3584. (in Chinese)

[11] Zheng D, Lin D, Song T. Research on disturbance rejection rate parasitic loop and its dynamics effect of strapdown imaging seeker[J]. ***Acta Armamentarii***, 2014, 35(11): 1774-1782. (in Chinese)

[12] Wang L, Xia Q, Qi Z. Effects of detector and rate gyro noise and scale-factor errors on systems using strap-down detector and integral form of proportional navigation law [J]. ***Acta Electronica Snica***, 2006, 34(9): 1653-1658. (in Chinese)

[13] Wang Z. Optimal State Estimation and System Identification [M]. Xi'an: Northwestern Polytechnical University Press, 2004. (in Chinese)

[14] Ananthasayanam M R, Sarkar A K, Vohra P. Estimation of LOS rates and angles using EKF from noisy seeker measurements [C]//International Conference on Signal Processing & Communications, 2004.

[15] Smita Sadhu, Ghoshal T K. Sight line rate estimation in missile seeker using disturbance observer-based technique[J]. ***IEEE Transactions on Control Systems Technology***, 2001, 19(2): 449-454. (in Chinese)

[16] Wang W, Lin D, Xu P. Strap-down seeker LOS angular rate estimation[J]. ***Infrared and Laser Engineering***, 2015, 44 (10): 3066-3069. (in Chinese)